COMSOL CONFERENCE 2024 FLORENCE

A 2D Computational Model of a ThermoMagnetic Device

Francisco Rodríguez-Méndez[1], Lorenzo Gallo[2,3], Francesco Cugini[3], Simone Fabbrici[2], Franca Albertini[2], Bruno Chinè[1]

1. School of Materials Science and Engineering, Costa Rica Institute of Technology, Cartago, Costa Rica
2. Institute of Materials for Electronics and Magnetism, National Research Council, Parma, Italy
3. Department of Mathematical, Physical and Computer Sciences, University of Parma, Italy.

Abstract

In this work, a two-dimensional time-dependent model of a ThermoMagnetic Energy Converter (TMEC) device is developed using COMSOL Multiphysics® for harvesting low-grade waste heat and converting it to useful and clean energy. The model consists of a rotor, a permanent magnet assembly, a heat source, and a heat sink. The rotor is made of $Ni_{48}Mn_{36}Sn_{16}$, a Heusler compound with magnetocaloric properties, and it spins in proximity to the magnetic field created by the magnets due to the abrupt change in the material magnetization when it undergoes a phase transformation as a result of heat exchange with the surroundings. Then, the thermal source is a hot water tank with the rotor partially in contact with the fluid, while the heat sink is the environment modeled as air. With this approach, the magnetic and kinetic responses of the system were studied, as well as its efficiency, where the mass magnetization of the magnetocaloric material is extrapolated from experimental measurements. The results show an irregular acceleration pattern caused by the gradual heating of the material and the surroundings, hence yielding a decreasing change in its magnetization, behavior observed in working prototypes as well. Nevertheless, this model encourages future approaches where different materials and working parameters can be varied, optimizing the overall response of the device.

Keywords: magnetocaloric materials, thermo-magnetic generator, computational modeling and simulation, heat transfer, low-grade heat, energy harvest.

Introduction

Reducing greenhouse gas emissions and finding new ecological and renewable energy sources are among the biggest challenges humanity is facing nowadays [1] [2]. At the same time, power requirements are increasing constantly, where primary energy consumption is intrinsically accompanied by thermal losses when converted into usable energy [3]. These energy losses are usually in the form of waste heat, which is often released into the atmosphere contributing to global warming [4]. Furthermore, almost 72% of the energy produced by primary energy sources is lost during conversion, where more than 45% of the losses are waste heat emitted at temperatures below 100 °C [5], being the most significant source of it the exhaust air from heating systems, e.g. burners, furnaces, dryers, and heat exchangers [6]. Utilizing these low-grade thermal energies and turning them back into a more functional form, such as mechanical or electric energy, has been subject of research in recent years.

To date, new technologies have been studied capable of harvesting low-grade waste heat, such as thermoacoustic and Stirling engines, thermoelectric and thermomagnetic generators, organic Rankine cycles, among others [7] [8] [9]. However, most of these mechanisms use expensive materials and they are characterized by low thermodynamic efficiencies for a 100 ºC heat source with a heat sink at 25 ºC, i.e. the environment, making the recovery process economically unviable. For instance, thermoelectric generators, which are currently the most popular low-temperature energy conversion devices, reached only 5% conversion efficiency [10]. Thermoacoustic and Stirling engines have demonstrated an efficiency lower than 5%, with high machining and assembly costs [11] [12]. Generators based on the Rankine cycle are also expensive or not efficient enough to be considered profitable for industrial applications [13]. Therefore, developing new approaches capable of efficiently and cost-effective converting low-grade waste heat into usable and clean energy is crucial.

As an environmental-friendly alternative with high potential, the Thermo-Magnetic Generation (TMG) is being studied to convert low-grade waste heat into suitable energy [14]. This approach is based on the use of magnetocaloric materials when they lose their magnetic properties at a critical temperature, known as the Curie temperature (T_c), where the spontaneous magnetization of the material drops to zero undergoing a phase transformation [6] as a result of heat exchange with the environment.

The influence of heat on the magnetic properties of ferromagnetic materials has been quite familiar for a long time. Several patents following the idea of using magnetic materials to convert heat into mechanical or electrical energy were issued in the late 19th century, when Nikola Tesla and Thomas Edison separately designed prototypes of thermo-magnetic generators [15] [16]. Unfortunately, the performance of these devices was very low, and no domestic or industrial applications were developed in this area. In recent decades, with the advances obtained in the

development of magnetic refrigeration devices, and the study of magnetocaloric materials (MCM), a fresh assessment of TMG has been explored again. Kitanovski et al. [17] conducted a comprehensive feasibility study for the Swiss Federal Office of Energy on magnetocaloric power generation, giving a positive outlook. Hsu et al. [18] evaluated the potential efficiency of thermomagnetic power generation using different ferromagnetic materials. The study focused on polycrystalline gadolinium (Gd) exposed to a magnetic field of 0.3T and a temperature shift of 5K, revealing a considerably energy efficiency of 30.4%. Post et al. [19] theoretically investigated the energy conversion efficiency of Heusler alloys, revealing an efficiency of 15.9% for an applied magnetic field of 0.3T, and 63.8% for an applied magnetic field of 1.5T. Ferreira et al. [20] performed a comprehensive numerical computational fluid dynamics (CFD) analysis on different magnetocaloric regenerator geometries for a thermomagnetic engine. Almanza et al. [21] [22] compared thermomagnetic and thermoelectric power generation and revealed TMG can be more efficient. The authors showed that it has a slightly higher power density than thermoelectric power generation for a temperature difference below 10K, concluding that harvesting low-grade thermal energy under the principle of thermomagnetic generation is feasible.

In this work, a two-dimensional time-dependent computational study of a Thermo-Magnetic Energy Converter (TMEC) is developed as a first approach to assess its magnetic and kinetic response. The model is based on the mechanical motor architecture, where the TMEC rotor is made of $Ni_{48}Mn_{36}Sn_{16}$, a Heusler compound with magnetocaloric properties. The simulation accounts for the behavior of the rotor angular velocity, the temperature gradient between the device components, and the magnetic response of the material. With the numerical results obtained, the efficiency of the system is then calculated.

Thermo-Magnetic Theory

To better understand the operation of a TMEC, first we describe a thermo-magnetic cycle. This generalized approach is based on equilibrium thermodynamics, where the MCM acts as the functional material with a transition temperature T_t, and a magnetization dependent on the magnetic field applied and the temperature $M(H,T)$. The cycle performs two isothermal transformations, where the system produces work, and two isofield transitions, where the converter exchanges heat with the surroundings. To account for this energy change in each phase, the total differential of the Gibbs free energy [23] is used as follows

$$dG = Vdp - SdT - \mu_0 MdH \qquad (1)$$

where V is the system volume, p is the pressure, S is the entropy, T is the temperature, μ_0 is the magnetic field constant, M is the magnetization, and H is the magnetic field strength. Knowing the process occurs at atmospheric pressure, the first term in Eq. 1 can be neglected, while the other terms change their values depending in the phase of the cycle. For instance, the four steps in a thermo-magnetic cycle are described below [24], where Fig. 1 also illustrate them.

1. **Step I** – the system starts at ambient temperature, where the MCM is below T_t and exhibits a high magnetization, or M_{cold}. At constant temperature, a magnetic field H is applied, which reduces the Gibbs energy of the MCM by $-\mu_0 M_{cold} H$.
2. **Step II** – low-grade waste heat Q_{in} is used to heat the MCM above T_t, which reduces the magnetization to M_{hot} and the Gibbs energy by $-S\Delta T$.
3. **Step III** – the magnetic field is removed while keeping the temperature constant, where just a low value of the Gibbs energy $+\mu_0 M_{hot} H$ is required for the system.
4. **Step IV** – the hot MCM is brought again into contact with the ambient temperature, which changes the Gibbs free energy by $S\Delta T$, restoring the magnetization to M_{cold}, returning the system to the state described in Step 1, closing the thermo-magnetic cycle.

The thermo-magnetic cycle described is implemented in several architectures of TMG devices, such as generators, oscillators and motors. Thermomagnetic motors, which is the approach followed in this work, are based on mechanical rotation. This mechanism uses a rotatable ring of a magnetocaloric material. Its rotation causes each part of the MCM to undergo the four stages of the thermodynamic cycle. In step I, the application of the magnetic field, produced by an array of permanent magnets, causes the MCM to be strongly attracted by the field gradient at the edge of the magnet. In step II, the magnetic material is heated by the low-grade waste heat, which reduces its magnetization to M_{hot}.

During step III, when the MCM leaves the magnetic field, only a low torque interferes with its rotation. In step IV, the temperature of the MCM reaches again the ambient temperature, restoring the high

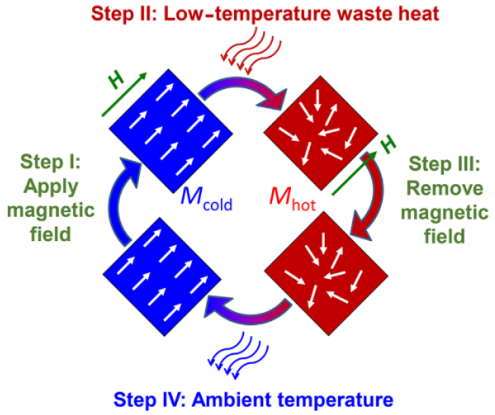

Figure 1. *Thermo-Magnetic cycle for harvesting low-grade waste heat. Obtained from [24].*

M_{cold}. The heat provided by the low-grade thermal source is employed to convert the magnetic energy $\mu_0 M_{hot} H$ into mechanical energy, which can be later transformed to electrical energy using a conventional generator. Particularly, the TMEC based on rotors show promising outcomes, e.g. the Swiss Blue Energy AG prototype, which reached a power of 1.4 kW, using gadolinium as MCM [25], or the rotor showed by Kishore et al. [8] achieving a high power density generation with a sharp efficient performance.

Generation of useful energy in quantities quite large is one the most promising characteristics of this technology, but only if the materials used meet several important aspects. For instance, MCMs must have excellent thermal properties, a considerable magnetization difference between the hot and cold working temperatures (i.e., the hot source and the heat sink, respectively), and to be cost-effective. In addition, and due to the temperature range required for TMG, the magnetocaloric material needs to have the right transition temperature T_t to maximize the system efficiency. Thus far, gadolinium has been the benchmark material for this kind of application showing good performance, it remains as a critically rare earth metal with low availability, high cost, and a fixed T_t, making it a non-viable option [26]. In the other hand, Heusler alloys are low cost, recyclable, highly available, and rare-earth free, making them an advantageous material for thermo-magnetic generation, also exhibiting a wide tunability of their critical temperatures and magnetic attributes, opening the possibility of tailoring their basic and functional properties by precise changes in their composition [27] [28].

TMEC Modeling

Given the output characteristics for the TMEC motor architecture, and the properties needed for the MCM, the model developed consists of a rotor, a permanent magnet assembly, a thermal source, and a heat sink. The rotor is made of $Ni_{48}Mn_{36}Sn_{16}$, a Ni-Mn-based Heusler alloy with its maximum magnetocaloric response in a temperature range close to its Curie transition ($T_c = 315K$). The rotor spins in proximity to the magnetic field created by a set of three permanent magnets and the abrupt change in the MCM magnetization when it undergoes a ferromagnetic-to-paramagnetic phase transformation as a result of heat exchange with the surroundings. The low-grade waste heat source is a hot water tank with the rotor partially in contact with the fluid, while the heat sink is the environment modeled as air. Fig. 2 shows a schematic of the TMG device described.

The model uses the Gauss' law for magnetic fields formulated in the COMSOL Multiphysics® AC/DC module under the Magnetic Fields, No Currents interface to describe the magnetostatic fields produced by the magnets array. The heat transfer and the enthalpy flow in the thermal source, the rotor, and the solid-fluid interface are solved using the energy

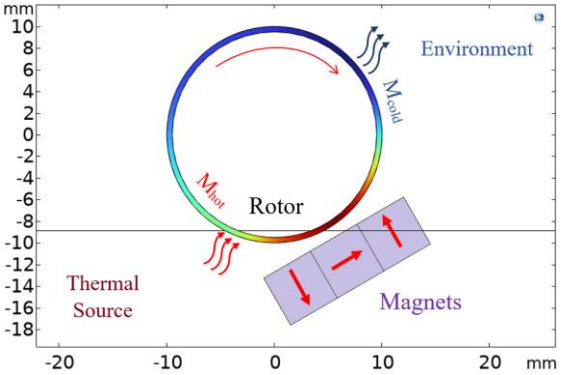

Figure 2. *TMEC model implemented.*

conservation equation given in the Heat Transfer in Solids and Fluids Physic. The mass magnetization of the magnetocaloric material is introduced to the model by defining an interpolated function based on experimental data, allowing the kelvin force yielded by the rotor to be calculated and later converted into angular acceleration by the means of a General Form PDE (Partial Differential Equations) interface, where the motion of the rotor is added using the Moving Mesh module with a Rotating Domain node.

Governing equations of the model

MCM magnetization is dependent on the intensity of the magnetic field $\boldsymbol{H}$ created by the magnets' array and the temperature $\boldsymbol{T}$ in the rotor. To calculate $\boldsymbol{H}$, in a current free region, where $\nabla x\boldsymbol{H} = 0$, it is possible to define a scalar magnetic potential V_m from

$$\boldsymbol{H} = -\nabla V_m \tag{2}$$

Then, using the following constitutive relations

$$\boldsymbol{B} = \mu_0(\boldsymbol{H} + \boldsymbol{M}) \tag{3}$$

$$\nabla \cdot \boldsymbol{B} = 0 \tag{4}$$

where $\boldsymbol{B}$ is the magnitude flux density, $\boldsymbol{M}$ is the magnetization of each of the permanent magnets, μ_0 is the vacuum permeability; an equation for V_m can be derived as

$$-\nabla \cdot (\mu_0 \nabla V_m - \mu_0 \boldsymbol{M}) = 0 \tag{5}$$

The governing equation that allows the calculation of the rotor temperature, along with the heat transfer interactions between the other TMEC components, in each step of the thermo-magnetic cycle, is the heat relation for conductive and convective heat transfer

$$\rho C_p \boldsymbol{u} \cdot \nabla T + \nabla \cdot (-k\nabla T) = Q_{in} \tag{6}$$

where C_p is the material specific heat capacity, T is the temperature, k is the thermal conductivity, ρ is the density, $\boldsymbol{u}$ is the velocity vector, and Q_{in} is the low-grade thermal source.

Knowing the magnetization of the MCM, along with its temperature and the magnetic field gradient, the kelvin force acting on the material can be estimated as follows

$$\boldsymbol{F} = \mu(\boldsymbol{M} \cdot \nabla)\boldsymbol{H} \tag{7}$$

where μ is the material relative permeability. Assuming $\boldsymbol{M}$ is parallel to $\boldsymbol{H}$ due to the soft ferromagnetic behavior MCM exhibits, Eq. 7 can be rewritten as

$$\boldsymbol{F} = \mu M \boldsymbol{\nabla} H \tag{8}$$

As the movement of the rotor is constrained and it can only rotate around its own axis, we can convert the Eq. 8 into polar coordinates and calculate the tangential component of the force alone, following the next relation

$$\boldsymbol{F} = \frac{1}{R}\mu M \frac{\partial H}{\partial \theta}\hat{\boldsymbol{u}}_t \tag{9}$$

where R is the radius coordinate, and $\hat{\boldsymbol{u}}_t$ represents the unit vector on the direction of the magnetic field gradient. Once the force has been calculated, the momentum of the system, considering only the tangential force to the rotor, is expressed as

$$\tau = r_{avg} F \tag{10}$$

where r_{avg} is the average radius of the rotor. Since the rotor can be treated as a rigid body, the motion of the system is solved using the rotational dynamics equation, which relates the resulting torque τ to the angular acceleration of the device as

$$\alpha = \frac{\tau}{I} \tag{11}$$

where I is the moment of inertia associated with the rotor of mass m, internal radius r_{in}, and external radius r_{ext}, described by the relation

$$I = \frac{1}{2} m (r_{ext}^2 + r_{in}^2) \tag{12}$$

Finally, given the angular acceleration α at the time t, the angular velocity is calculated with the equation of rotational kinetics as follows

$$w(t) = w(t - dt) + \alpha(t) dt \tag{13}$$

Boundary conditions and design parameters of the TMEC model

$Ni_{48}Mn_{36}Sn_{16}$ magnetization $M(T, H)$ measurements were conducted with a stationary pendulum magnetometer, varying the magnetic field H from 0 T to 0.7 T at temperature values ranging from 269 K to 357 K. The extrapolated curves obtained are displayed in Fig. 3. Other model relevant properties of the MCM Heusler compound are summarized in Table 1. Also, the permanent magnets are made of NdFeB with a magnetization of 900 kA/m, following the magnetic flux direction shown in Fig. 2.

Table 1. *$Ni_{48}Mn_{36}Sn_{16}$ Heusler alloy properties.*

Parameter	Value
Magnetic permeability	1.237e^{-6} N/A^2
Thermal conductivity	20 W/(m·K)
Heat capacity	500 J/(kg·K)
Material density	7900 kg/m^3
Rotor total mass	3 g

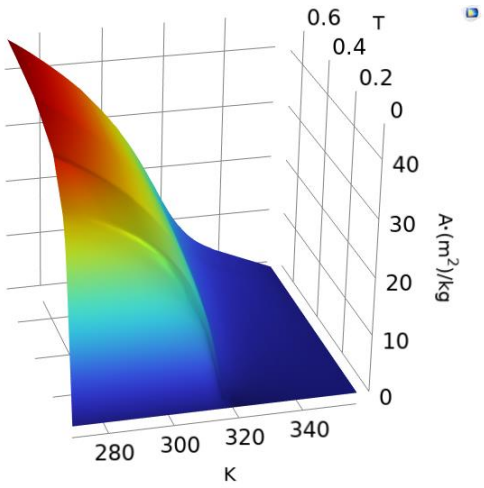

Figure 3. *$Ni_{48}Mn_{36}Sn_{16}$ magnetization per unit mass.*

The geometrical configuration implemented in the model is given in Table 2. As illustrated in Fig. 2, only 10% of the rotor surface is submerged into the water tank. To maximize the magnetic field gradient in the solid-fluid interface, where the rotor enters contact with the thermal source, the magnets array is 1mm away from the rotor, shifted with a 300º angle anticlockwise.
Temperatures for the low-grade thermal source and the air domain were set to 333.15 K and 293.15 K, respectively, where the water tank temperature was fixed throughout the study.

Table 1. *Geometrical configuration of the model.*

Part	Dimensions
Side length of a single magnet	20 mm
Rotor - external radius	10 mm
Rotor - internal radius	9.5 mm
Low-grade thermal source	20 x 60 mm^2
Air domain	60 x 50 mm^2

Efficiency of the TMEC

Thermodynamic efficiency is the key parameter of every energy harvesting process. It is defined as the fraction of usable output energy versus thermal input energy Q_{in} during each cycle. For TMG, the material efficiency follows the relation

$$\eta = \frac{\mu_0 (M_{cold} - M_{hot}) H}{Q_{in}} \tag{14}$$

Simulation Results and Discussion

A time-dependent study was carried out for 120s, where computational results for the magnetic field generated by the magnets array, the behavior of the rotor angular velocity, the temperature gradient along the rotor's surface, the change in the magnetization of the MCM, and the efficiency of the TMEC are then obtained for the system implemented.
The magnetic field generated by the permanent magnets array is shown in Fig. 4, where the maxi-

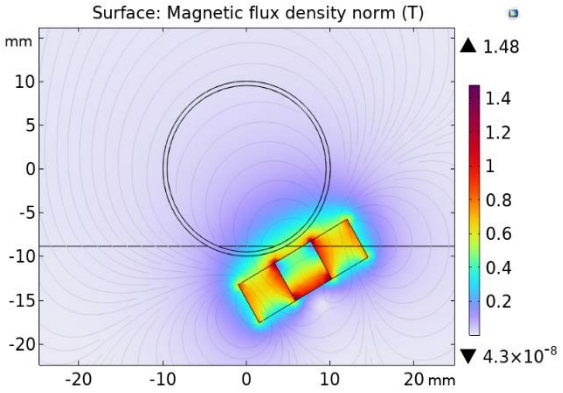

Figure 4. *Magnetic Field generated by magnets array.*

mum value achieved in the solid-fluid interface, where the rotor enters contact with the waste-heat thermal source, was 0.69 T. This value determines also the peak magnetization change the MCM can accomplish, as it is illustrated back in Fig. 2, where the coloring in the rotor displays the spatial change in the intensity of the material magnetization depending on the temperature, being the values of red the low magnetization M_{hot} at high temperature, while the blue grades represent the high magnetization M_{cold} at lower temperatures.

With the material magnetization also depending on temperature, Fig. 5 shows the behavior over time of the temperature at four different angles of the rotor, while Fig. 6 displays a comparison of the system temperature at two different times: at the beginning of the study, and in the final time step. The curves obtained in Fig. 5 indicate the gradual heating of the rotor with little temperature change between the four positions, exposing the fact that the heat lost to the ambient during the cycle is not sufficient to cool down the material to its initial temperature, which progressively reduces the magnetization change when the MCM enters the magnetic field in the subsequent cycle. Besides, this behavior directly affects the velocity and the time in which the rotor completes a cycle, as the angular motion is heavily dependent on the magnetic force produced. Moreover, Fig. 6 shows how the low-grade thermal source heats up the air domain over the duration of the simulation, which also contributes to decrease the temperature gradient along the rotor, further

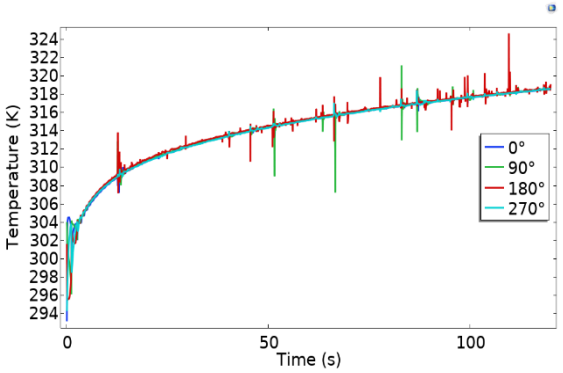

Figure 5. *Temperature gradient at different angles along the MCM rotor.*

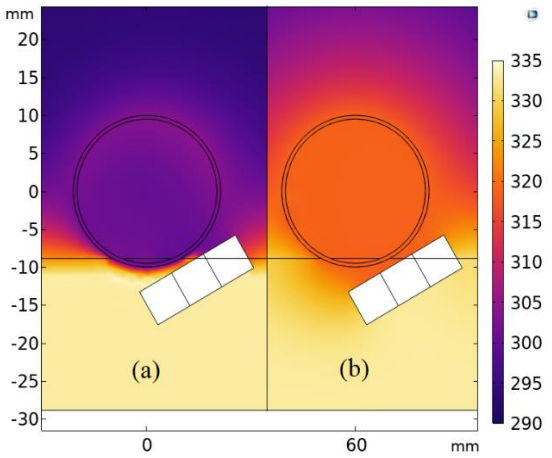

Figure 6. *Temperature profile over the TMEC model at (a) 2.5s, and (b) 120s.*

reducing its magnetization change. This issue is also observed in working prototypes [29]. Several strategies could address this problem, e.g. new magnetocaloric materials with better tailored thermal properties, i.e. low specific heat capacity and high thermal conductivity, allowing the MCM to rapidly exchange heat. Or considering the addition of other heat transfer mechanisms between the air domain and the MCM, such as a cold air fluid flow over the rotor, which allows the material to cool-down faster. Also, including a non-thermal conducting material in the air-water interface to improve the isolation between the ambient and the thermal source could prevent the heating of the entire system. Another option is to optimize the surface-to-volume ratio of the rotor or the percentage of material under the water.

Fig. 7 displays the difference in the magnetization between two points along the rotor: the first one located in the MCM-water interface, accounting for M_{hot}; while the point for M_{cold} was placed in the exact opposite position to the first point. Selection of these two points assures the maximum change in the magnetization the material is able of experiencing. The results obtained restate the fact that the change in the material magnetization reduces its value as the time goes by, due to the increasing temperature of the rotor consequence of the low rate of heat exchanged during the isofield II and IV transitions

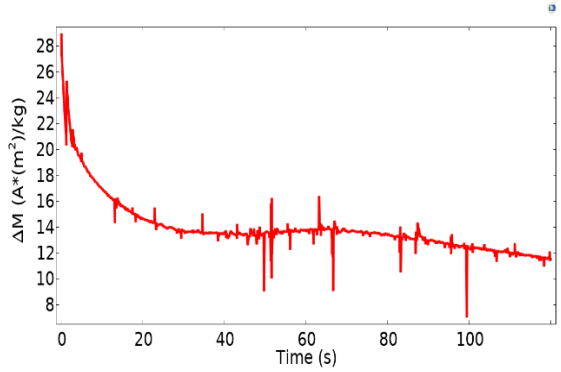

Figure 7. *Change in the $Ni_{48}Mn_{36}Sn_{16}$ rotor magnetization per unit mass over time.*

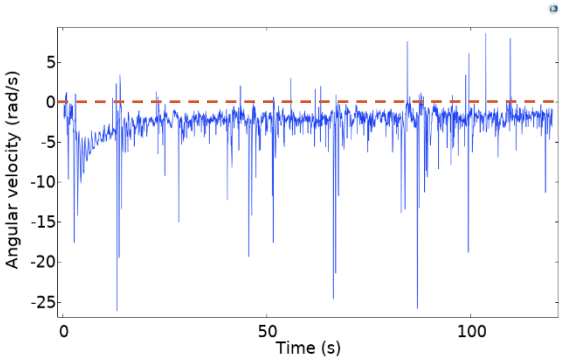

Figure 8. *Rotor angular velocity over time.*

while performing the thermo-magnetic cycle.
Accordingly with the temperature and the magnetization outcomes for the $Ni_{48}Mn_{36}Sn_{16}$ Heusler alloy, the rotor angular velocity shows the behavior given in Fig. 8, where the negative values obtained only indicate that the rotor has a counterclockwise movement. It is worth noting that, when the rotor has a large change in its magnetization (in the first 20s of the study, approximately) the rotor also achieved its best average angular velocity, with a maximum value of 26.137 rad/s. From that point on, the rotor velocity starts to decrease, reaching an average value close to 1.532 rad/s at the end of the time evaluated. Certain oscillations are observed throughout the rotor movement, where the direction of its rotation changes clockwise, but for a moment. These disturbances can be explained by comparing the spikes in the graphs for the material temperature and magnetization in Figs. 5 and 7, where these distortions coincide closely with the abrupt variations in the rotor velocity.
To evaluate the system efficiency, the performance metric proposed in Eq. 14 can be calculated using the results obtained for the magnetic field generated by the magnets array, the change in the magnetization of the $Ni_{48}Mn_{36}Sn_{16}$ magnetocaloric material, and the computation of Q_{in} by integrating the total heat flux over the low-grade thermal source domain. An efficiency of 4,41% was calculated for the TMEC modeled. Despite the seemingly low value yielded, the benchmark for this application is the Carnot efficiency [24] that follows the relation

$$\eta_{Carnot} = \frac{\Delta T}{T_{hot}} \qquad (15)$$

which represents the upper theoretical limit according to equilibrium thermodynamics. Taking $\Delta T = 40K$ and $T_{hot} = 333.15K$, the $\eta_{Carnot} = 12.007\%$. Then, the efficiency obtained for the TMEC is about 36.6% of the benchmark upper limit, which still can compete with thermoelectric generation.

Conclusions

This work presents a two-dimensional model of a Thermo-Magnetic Energy Converter based on the mechanical motor approach for harvesting low-grade waste heat. The system uses the $Ni_{48}Mn_{36}Sn_{16}$ Heusler compound as the functional material with magnetocaloric properties. The simulations show a magnetic and kinetic behavior somewhat undesirable as a result of two situations. First, the MCM heat exchange with the ambient is insufficient to decrease the rotor temperature before it enters the magnetic field in each cycle. Second, the low-grade thermal source also heats up the air domain, progressively increasing the temperature of the rotor. These issues produce a considerable reduction in the magnetization of the material, hence yielding a low conversion efficiency. However, the efficiency value calculated allows this device to be a promising alternative to current harvesting technologies.
Nevertheless, the results obtained have provided a valuable insight into the magnetic device behavior, which encourages future studies where other magnetocaloric materials and heat exchange strategies can be assessed, or the working parameters of the model can be varied to optimize its response, and therefore enhance its conversion efficiency. Following this path, the computational model developed could be used as a robust baseline to later improve the experimental work. Also, as the next natural iteration of the model, the force and rotational motion produced by the rotor can be subsequently converted into mechanical or electrical energy, allowing the validation of several other performance metrics of the thermomagnetic device.

Acknowledgements

The first and last author gratefully acknowledge the financial aid provided by the Vicerrectoría de Investigación y Extensión of the Instituto Tecnológico de Costa Rica, through the project 5402-1351-2301.

References

[1] D. Champier, "Thermoelectric generators: A review of applications," *Energy Conversion and Management*, vol. 140, pp. 167-181, 2017.

[2] M. Araiz, Á. Casi, L. Catalán, Á. Martínez and D. Astrain, "Prospects of waste-heat recovery from a real industry using thermoelectric generators: Economic and power output analysis," *Energy Conversion and Management*, vol. 205, 2020.

[3] M. Araiz, A. Martínez, D. Astrain and P. Aranguren, "Experimental and computational study on thermoelectric generators using thermosyphons with phase change as heat exchangers," *Energy Conversion and Management*, vol. 137, pp. 155-164, 2017.

[4] N. Jaziri, A. Boughamoura, J. Müller, B. Mezghani, F. Tounsi and M. Ismail, "A comprehensive review of Thermoelectric Generators: Technologies and common applications," *Energy Reports*, vol. 6, pp. 264-287, 2020.

[5] C. Formann, I. K. Muritala, R. Pardemann and B. Meyer, "Estimating the global waste heat potential," *Renewable and Sustainable Energy Reviews*, vol. 57, pp. 1598-1579, 2016.

[6] S. Hur, S. Kim, H.-S. Kim, A. Kumar, C. Kwon, J. Shin, H. Kang, T. H. Sung, J. Ryu, J. M. Baik and H.-C. Song, "Low-grade waste heat recovery scenarios: Pyroelectric, thermomagnetic, and thermogalvanic thermal energy harvesting," *Nano Energy*, vol. 114, p. 108596, 2023.

[7] R. Kishore and S. Priya, "A review on low-grade thermal energy harvesting: Materials, methods and devices," *Materials*, vol. 11, p. 1433, 2018.

[8] R. A. Kishore, B. Davis, J. Greathouse, A. Hannon, D. E. Kennedy, A. Millar, D. Mittel, A. Nozariasbmarz, M. G. Kang, H. B. Kang, M. Sanghadasa and S. Priya, "Energy scavenging from ultra-low temperature gradients," *Energy Environ Sci*, vol. 12, no. 3, pp. 1008-18, 2019.

[9] A. Bucsek, W. Nunn, B. Jalan and R. D. James, "Direct Conversion of Heat to Electricity Using First-Order Phase Transformations in Ferroelectrics," *Phys Rev Appl*, vol. 12, no. 3, 2019.

[10] R. A. Kishore and S. Priya, "A review on design and performance of thermomagnetic devices," *Renewable and Sustainable Energy Reviews*, vol. 81, pp. 33-44, 2018.

[11] T. Jin, R. Yang, Y. Wang, Y. Feng and K. Tang, "Low temperature difference thermoacoustic prime mover with asymmetric multi-stage loop configuration," *Scientific Reports*, vol. 7, p. 7665, 2017.

[12] K. Wang, S. R. Sanders, S. Dubey, F. H. Choo and F. Duan, "Stirling cycle engines for recovering low and moderate temperature heat: A review," *Renewable and Sustainable Energy Reviews*, vol. 62, pp. 89-108, 2016.

[13] O. Aboelazayem, M. Gadalla, I. Alhajri and B. Saha, "Advanced process integration for supercritical production of biodiesel: Residual waste heat recovery via organic Rankine cycle (ORC)," *Renewable Energy*, vol. 164, pp. 433-443, 2021.

[14] V. Srivastava, Y. Song, K. Bhatti and R. D. James, "The Direct Conversion of Heat to Electricity Using Multiferroic Alloys," *Advanced Energy Materials*, vol. 1, no. 1, pp. 97-104, 2011.

[15] N. Tesla, "Thermo-magnetic motor". U.S. Patent 396121A, 1889.

[16] T. A. Edison, "Pyromagnetic motor". U.S. Patent 380100A, 1888.

[17] A. Kitanovski, M. Diebold, D. Vuarnoz, C. Gonin and P. W. Egolf, "Applications of Magnetic Power Production and Its Assessment–A Feasibility Study," Swiss Federal Office of Energy, Bern, Switzerland, 2008.

[18] I.-K. Hsu, M. T. Pettes, M. Aykol, C.-C. Chang, W.-H. Hung, J. Theiss, L. Shi and S. B. Cronin, "Direct observation of heat dissipation in individual suspended carbon nanotubes using a two-laser technique," *Journal of Applied Physics*, vol. 110, no. 4, p. 044328, 2011.

[19] A. Post, C. Knight and E. Kisi, "Thermomagnetic energy harvesting with first order phase change materials," *Journal of Applied Physics*, vol. 114, no. 3, p. 033915, 2013.

[20] L. Ferreira, C. Bessa, I. d. Silva and S. Gama, "A heat transfer study aiming optimization of magnetic heat exchangers of thermomagnetic motors," *International Journal of Refrigeration*, vol. 37, pp. 209-214, 2014.

[21] M. Almanza, A. Pasko, A. Bartok, F. Mazaleyrat, M. Lobue and Cachan, "Thermal energy harvesting thermomagnetic versus thermoelectric generator," in *7th Int. Conf. Magnetic Refrigeration at Room Temperature (Thermag VII)*, International Institute of Refrigeration (IIF/IIR), Paris 2016, 2016.

[22] M. Almanza, A. Pasko, F. Mazaleyrat and M. LoBue, "Numerical study of thermomagnetic cycle," *Journal of Magnetism and Magnetic Materials*, vol. 426, pp. 64-69, 2017.

[23] A. M. Tishin and Y. I. Spichkin, The Magnetocaloric Effect and its Applications, Bristol, UK: Institute of Physics Publishing, 2003.

[24] D. Dzekan, A. Waske, K. Nielsch and S. Fähler, "Efficient and affordable thermomagnetic materials for harvesting low grade waste heat," *APL Materials*, vol. 9, p. 011105, 2021.

[25] B. Vogel, "Electricity from low temperature waste heat," BFE-article, 2022.

[26] A. Kitanovski, "Energy Applications of Magnetocaloric Materials," *Advanced Energy Materials*, vol. 10, p. 1903741, 2020.

[27] F. Albertini, M. Solzi, A. Paoluzi and L. Righi, "Magnetocaloric properties and magnetic anisotropy by tailoring phase transitions in NiMnGa alloys," *Materials Science Forum*, vol. 583, pp. 169-196, 2008.

[28] M. Gueltig, F. Wendler, H. Ossmer, M. Ohtsuka, H. Miki, T. Takagi and M. Kohl, "High-performance thermomagnetic generators based on heusler alloy films," *Advanced Energy Materials*, vol. 7, no. 5, p. 1601879, 2017.

[29] L. Gallo, "Conversione termomagnetica di energia basata su materiali magnetici allo stato solido," Università degli Studi di Parma, Parma, Italia, 2020.